

# Enabling Nonlinear Manifold Projection Reduced-Order Models by Extending Convolutional Neural Networks to Unstructured Data



SHTC 2020

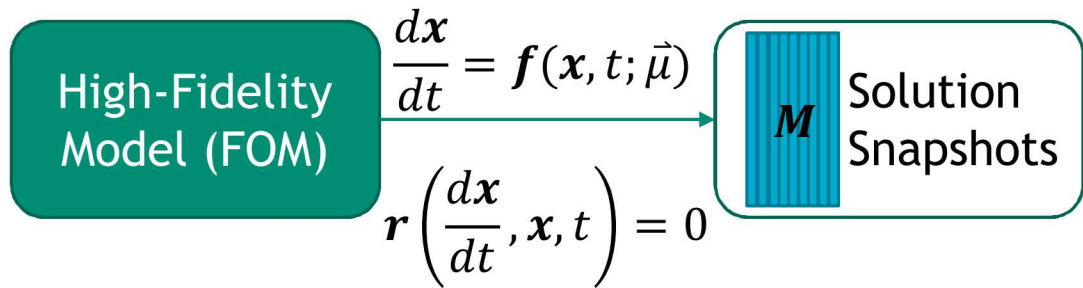
John Tencer and Kevin Potter



Supported by the Laboratory Directed Research and Development program at Sandia National Laboratories, a multimission laboratory managed and operated by National Technology and Engineering Solutions of Sandia LLC, a wholly owned subsidiary of Honeywell International Inc. for the U.S. Department of Energy's National Nuclear Security Administration under contract DE-NA0003525.

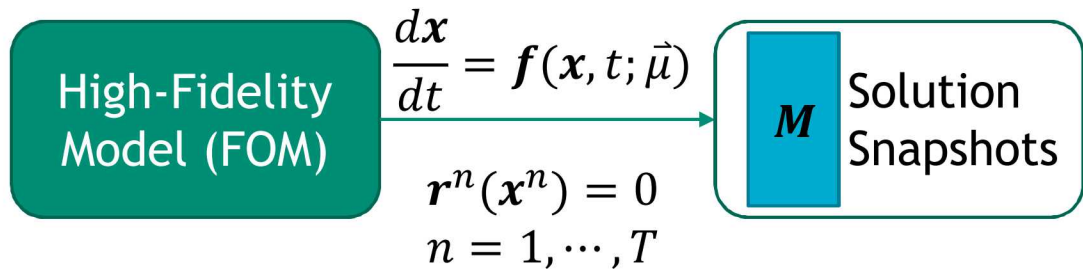
# Classical Model Reduction Overview

Generate Solution Snapshots

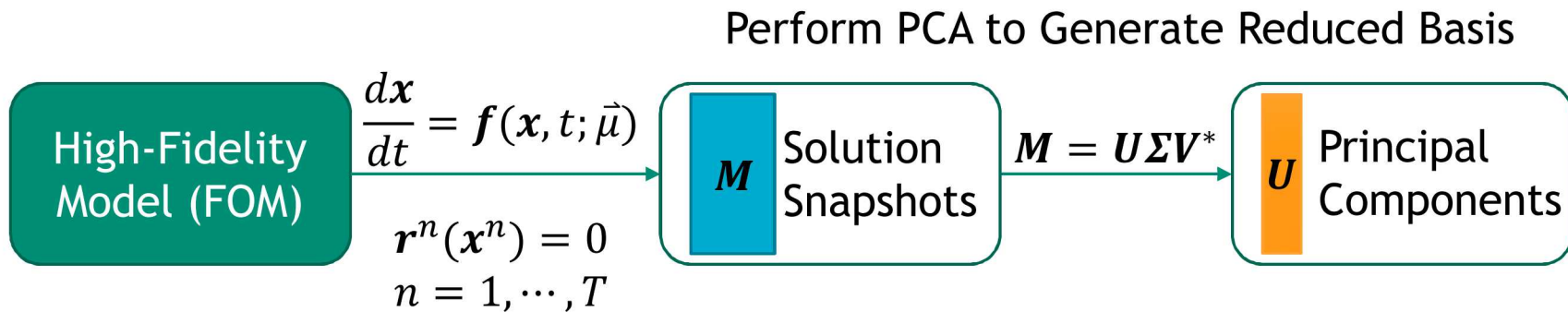


# Classical Model Reduction Overview

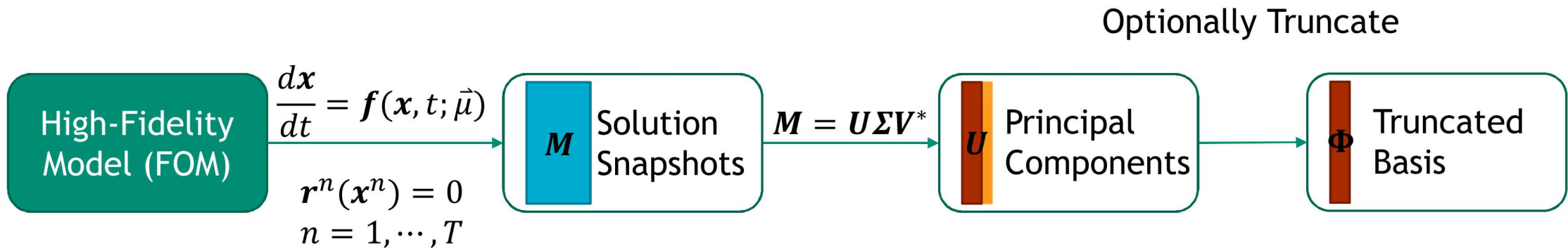
Generate Solution Snapshots



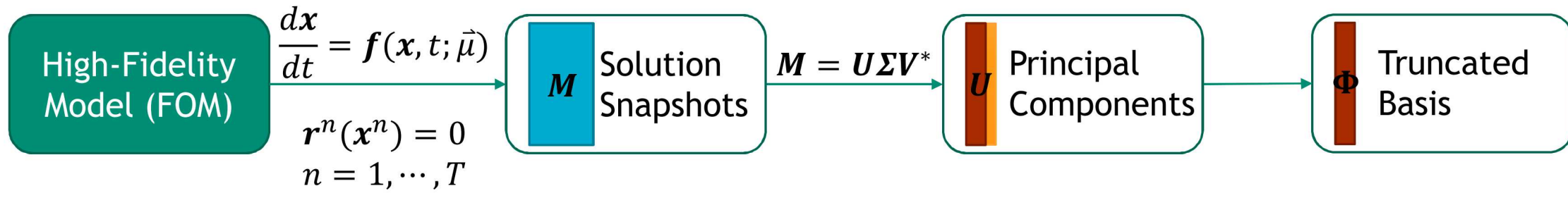
# Classical Model Reduction Overview



# Classical Model Reduction Overview

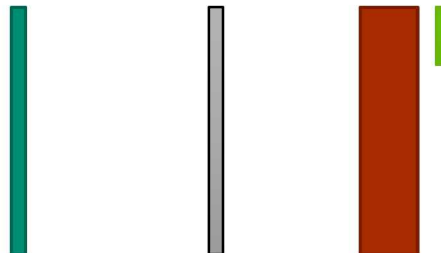


# Classical Model Reduction Overview

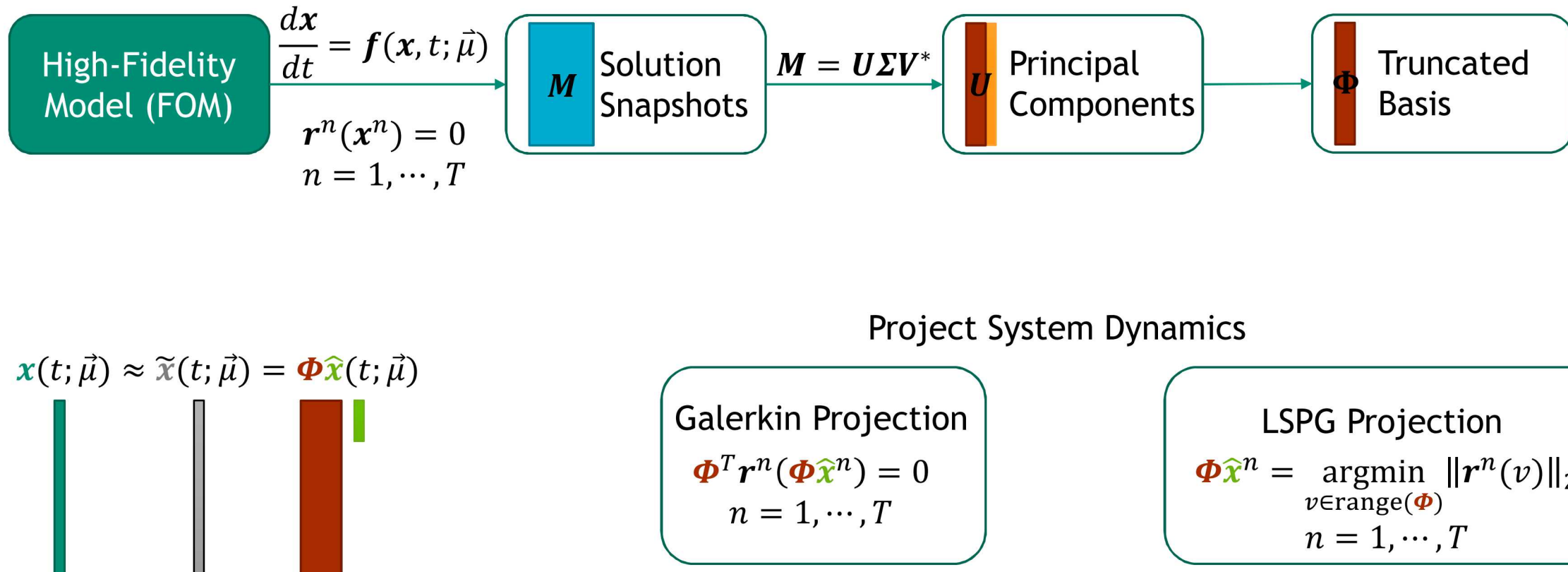


Approximate FOM State

$$\textcolor{teal}{x}(t; \vec{\mu}) \approx \tilde{x}(t; \vec{\mu}) = \Phi \hat{x}(t; \vec{\mu})$$

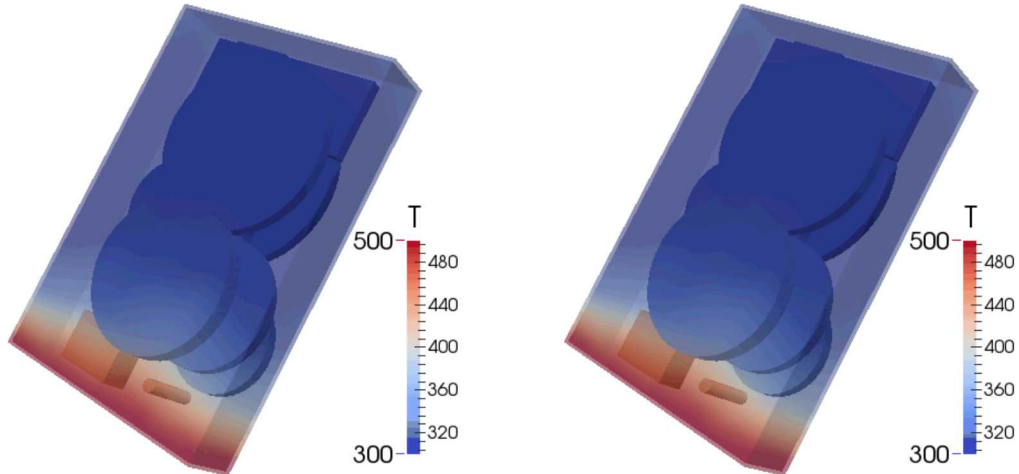


# Classical Model Reduction Overview

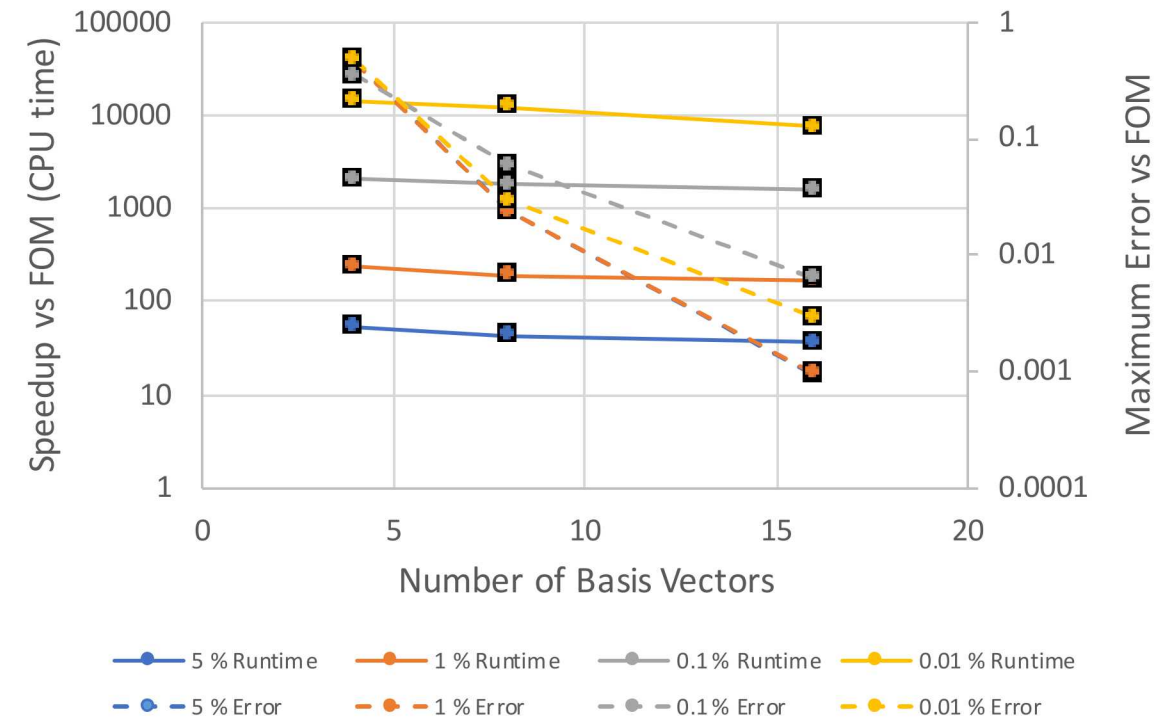


# Highly effective for diffusion dominated problems

- ROM methods are highly effective at reducing cost in (nonlinear) conduction problems.
- Easily applied to complex geometries.
- Hyper-reduction promises further performance benefits.



Comparison between FOM (left) and ROM (right) with only 4 modes retained.



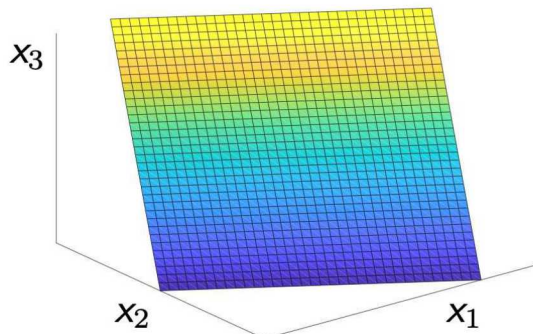
# Kolmogorov-width limitation



- ❖ Linear trial subspace sufficient for problems where the singular values of  $\mathbf{M}$  decay rapidly (i.e. diffusion dominated problems).
- ❖ For other problems the singular values decay slowly and many of the columns from  $\mathbf{U}$  are required to be retained in  $\Phi$  to achieve accurate solutions.
- ❖ ROM computational cost is closely tied to the number of modes retained
  - Newton-Raphson iteration costs scale quadratically with the trial subspace dimension

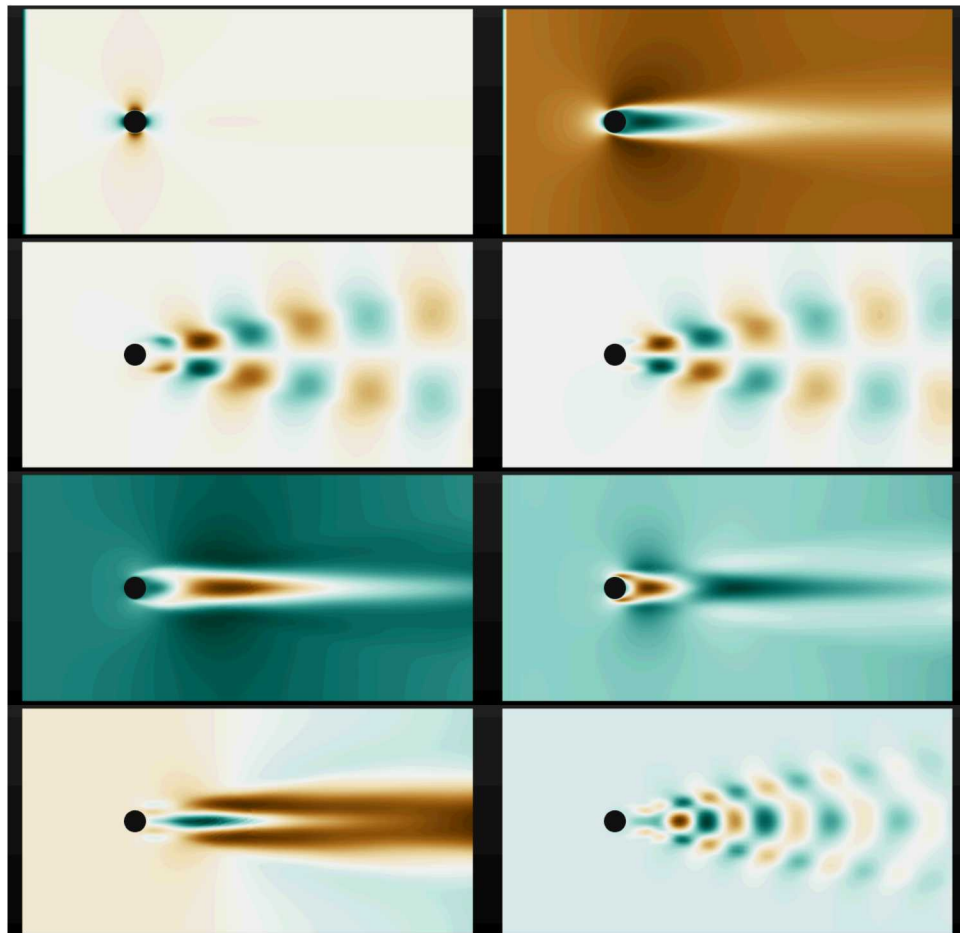
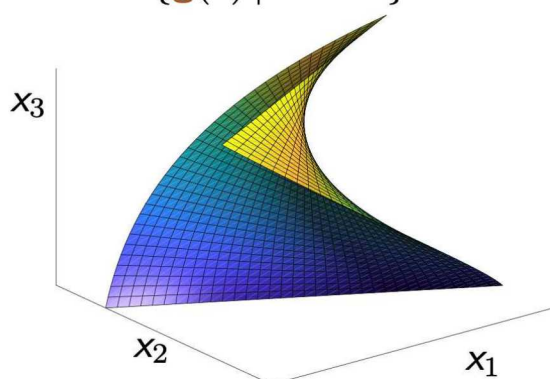
## Linear trial subspace

$$\text{range}(\Phi) := \{\Phi \hat{\mathbf{x}} \mid \hat{\mathbf{x}} \in \mathbb{R}^p\}$$

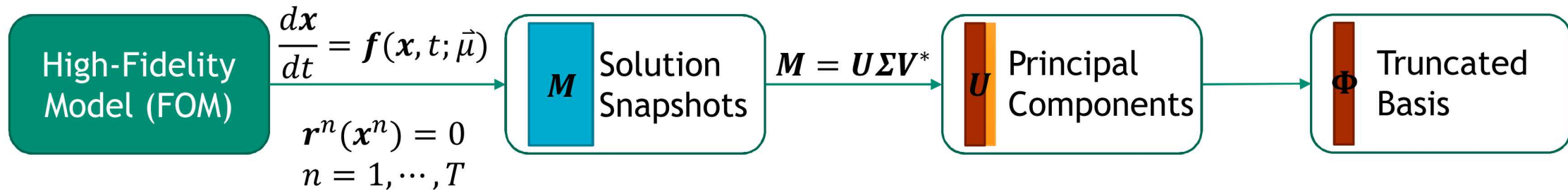


## Nonlinear trial manifold

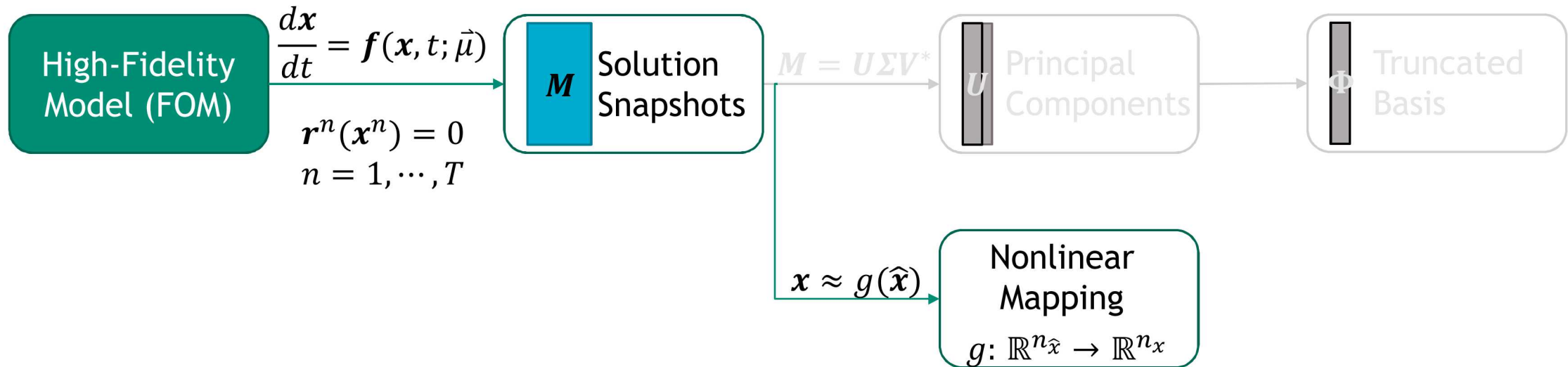
$$\mathcal{S} := \{\mathbf{g}(\hat{\mathbf{x}}) \mid \hat{\mathbf{x}} \in \mathbb{R}^p\}$$



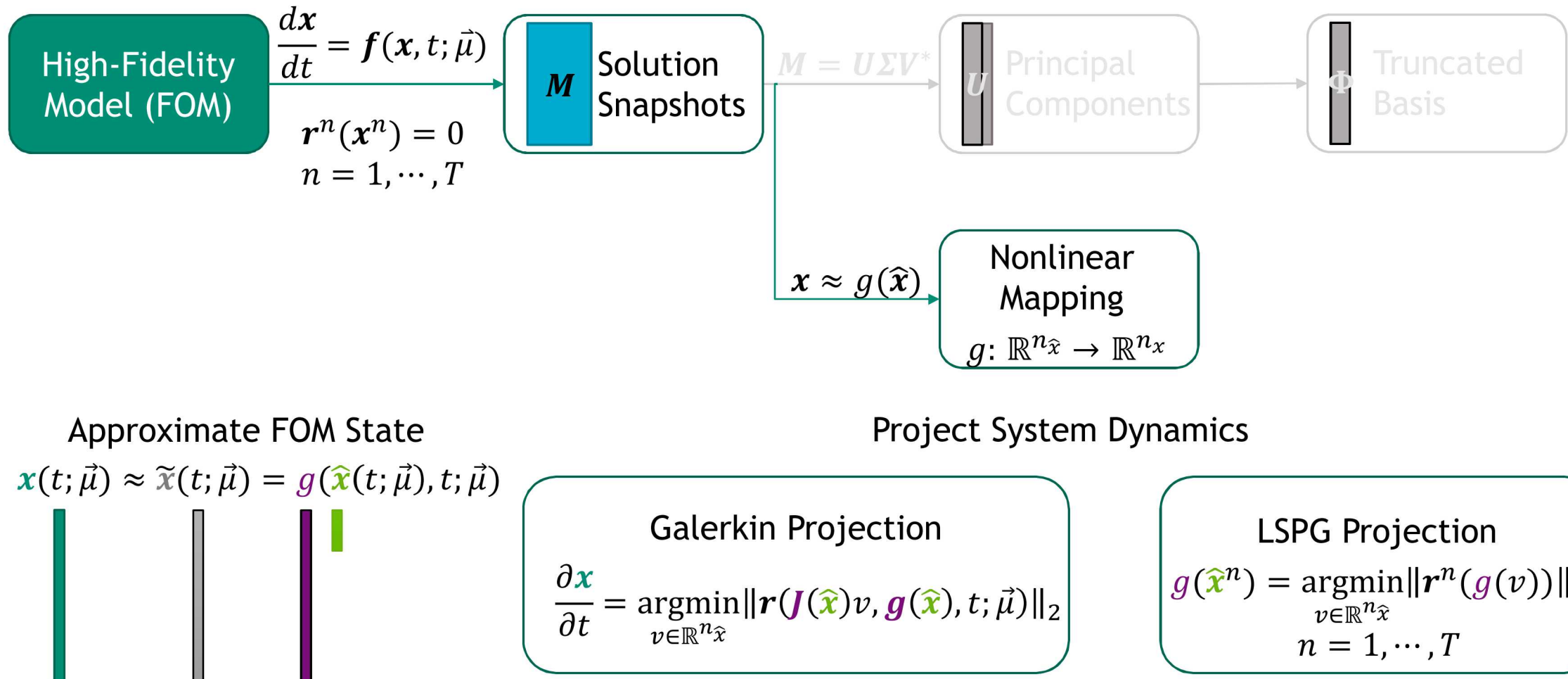
# Nonlinear Model Reduction Overview



# Nonlinear Model Reduction Overview

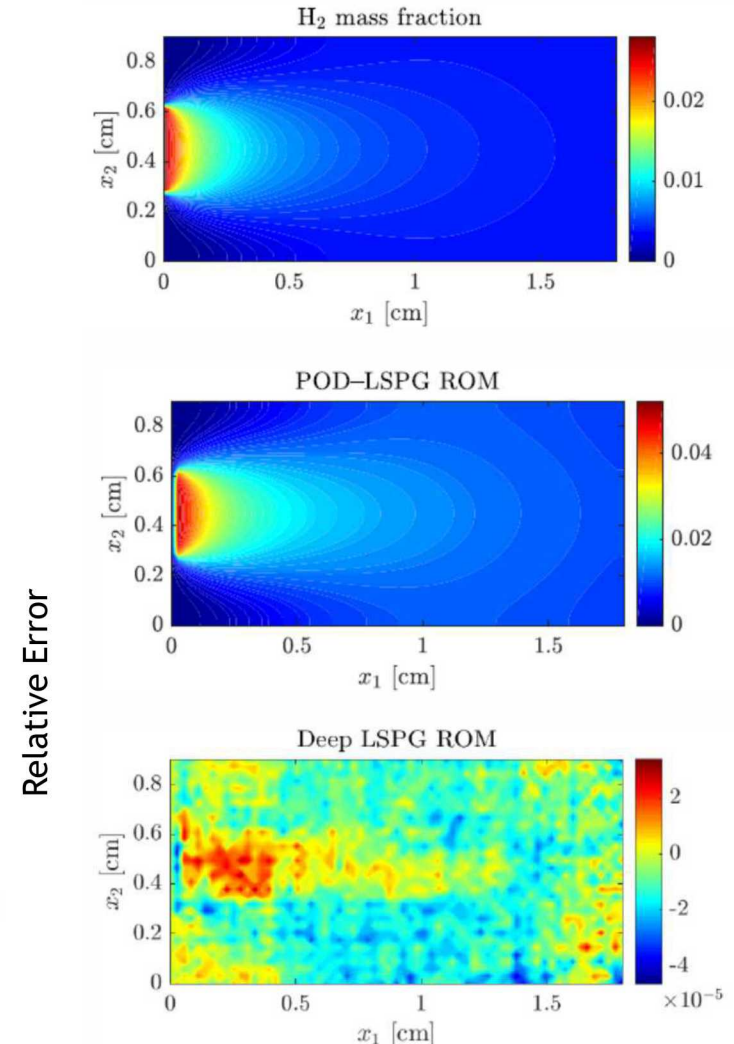
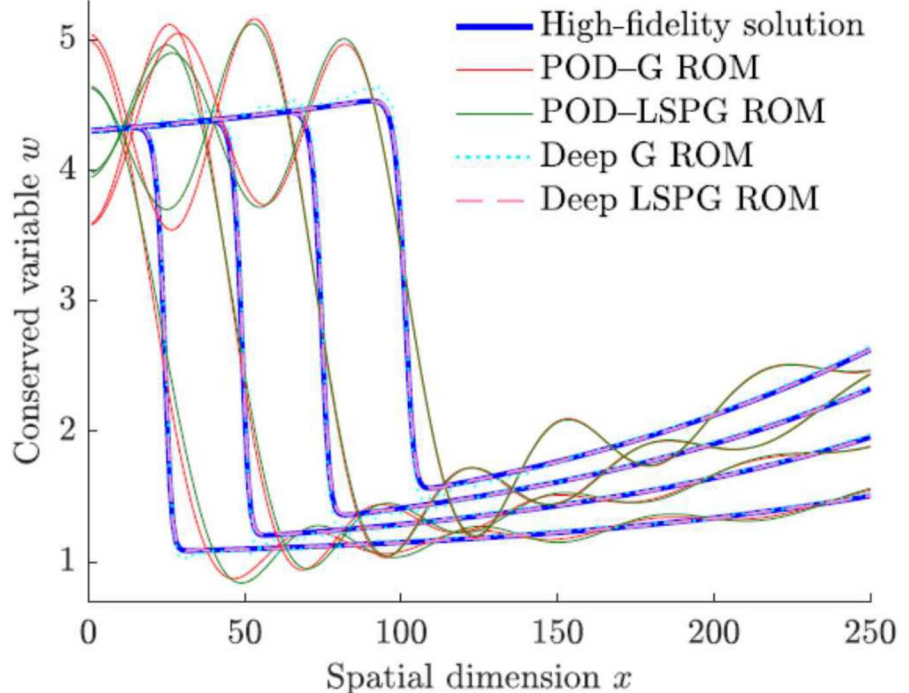


# Nonlinear Model Reduction Overview



# Manifold Projection ROMs

For advection dominated flows, nonlinear manifold projection techniques have been shown to consistently outperform linear subspace methods.



## How to generate nonlinear manifold?

K. Lee and K. Carlberg, *Model reduction of dynamical systems on nonlinear manifolds using deep convolutional autoencoders*, 2018

# Autoencoders for Manifold Learning

Unsupervised learning method

$$h: x \mapsto h_{dec}(h_{enc}(x))$$

Two parts:

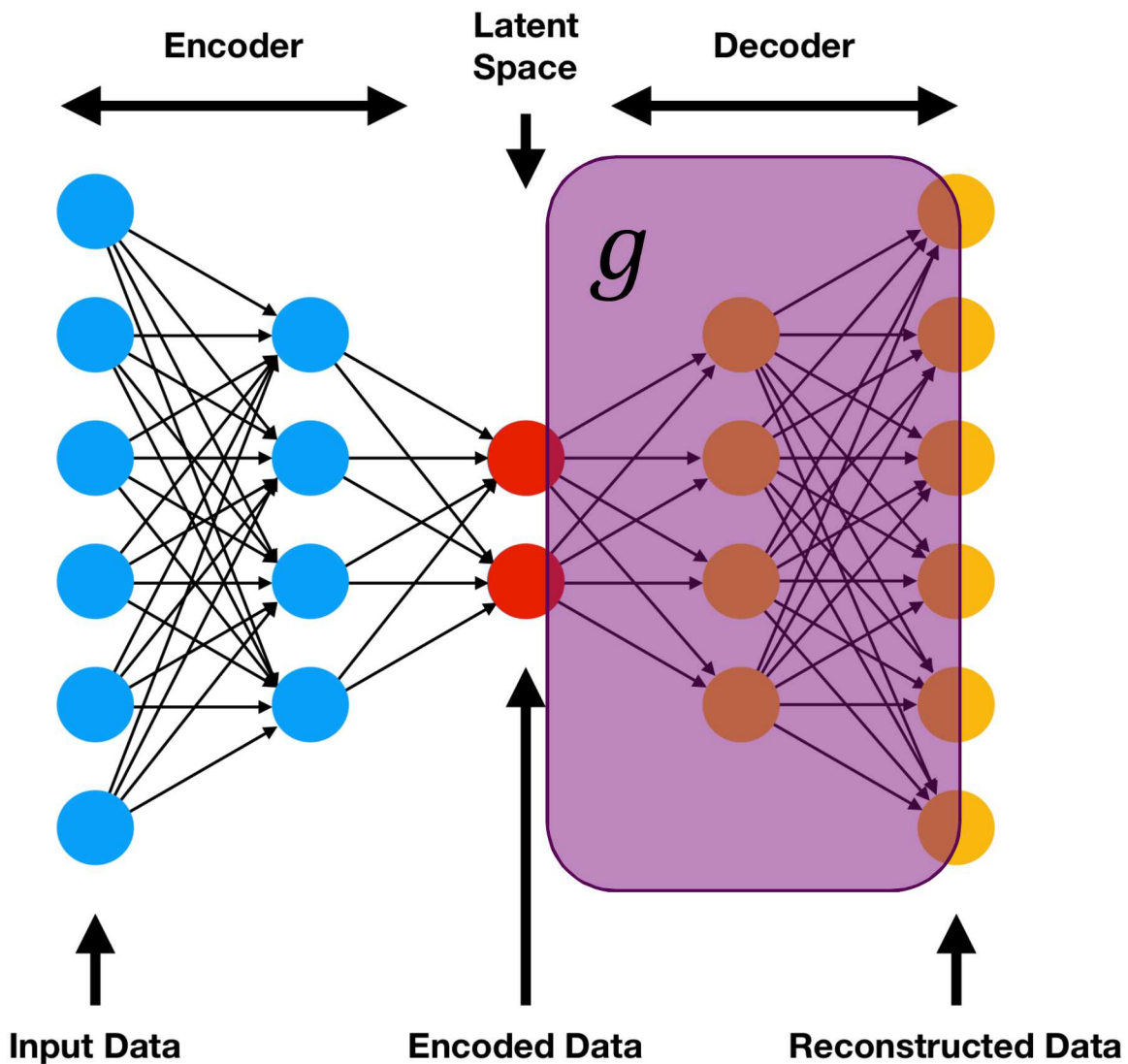
Encoder  $h_{enc}: \mathbb{R}^{n_x} \rightarrow \mathbb{R}^{n_{\hat{x}}}$

Decoder  $h_{dec}: \mathbb{R}^{n_{\hat{x}}} \rightarrow \mathbb{R}^{n_x}$

Each layer consists of a dense matrix-vector product and a non-linear activation function.

Large state space dimension ( $\mathbb{R}^{n_x}$ ) leads to impractically large number of parameters.

**Restricted to small states**



# Convolutional Autoencoders



Network architecture common in computer vision.

Reduces cost by sharing learned weights across the domain.

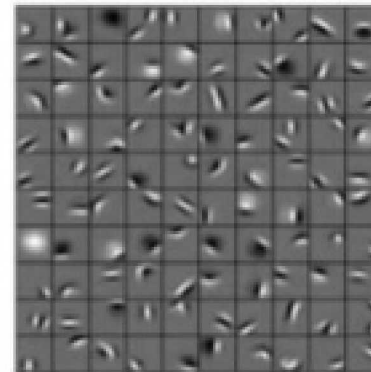
Matrix products are now sparse rather than dense.

0	0	0	0	0	0	0	0
0	60	113	56	139	85	0	0
0	73	121	54	84	128	0	0
0	131	99	70	129	127	0	0
0	80	57	115	69	134	0	0
0	104	126	123	95	130	0	0
0	0	0	0	0	0	0	0

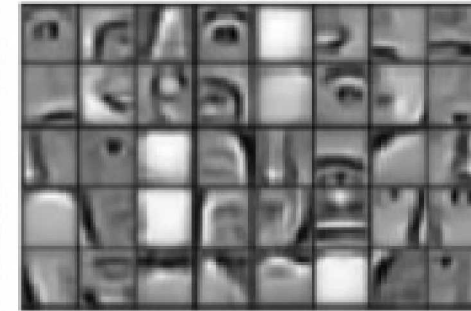
Kernel		
0	-1	0
-1	5	-1
0	-1	0

114				

Low-level feature



Mid-level feature



High-level feature



Source : Deep Learning in a Nutshell: Core Concepts, Nvidia  
<https://devblogs.nvidia.com/parallelforall/deep-learning-nutshell-core-concepts/>

**Restricted to structured data**

# Convolutional Layers for Unstructured Data

Commonly learned filters are often closely related to differential operators

$\nabla_x$		
-1	0	1
-4	0	4
-1	0	1

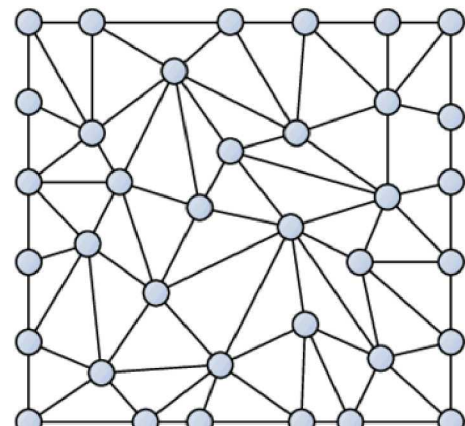
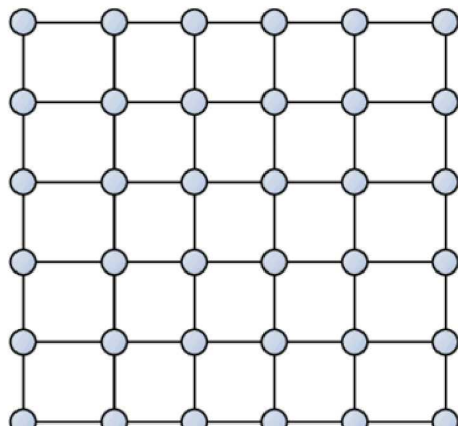
x- Sobel Filter

$\nabla_y$		
1	4	1
0	0	0
-1	-4	-1

y- Sobel Filter

$\Delta$		
-1	-1	-1
-1	8	-1
-1	-1	-1

Edge Detection



Use differential operators defined by the underlying spatial discretization to propagate information.

Operators can be computed offline or on-the-fly.

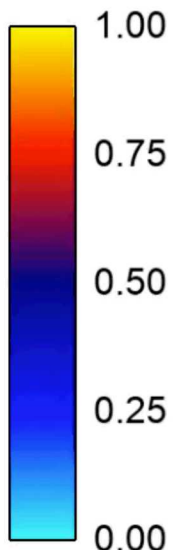
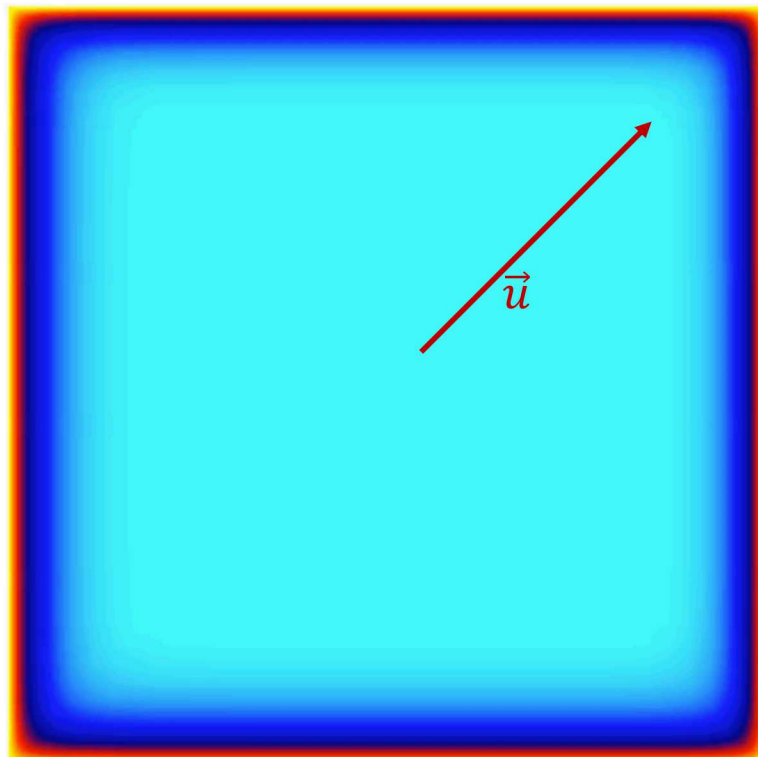
Resulting learned weights will be discretization independent.

Drop-in replacement for convolutional layers in autoencoder networks.

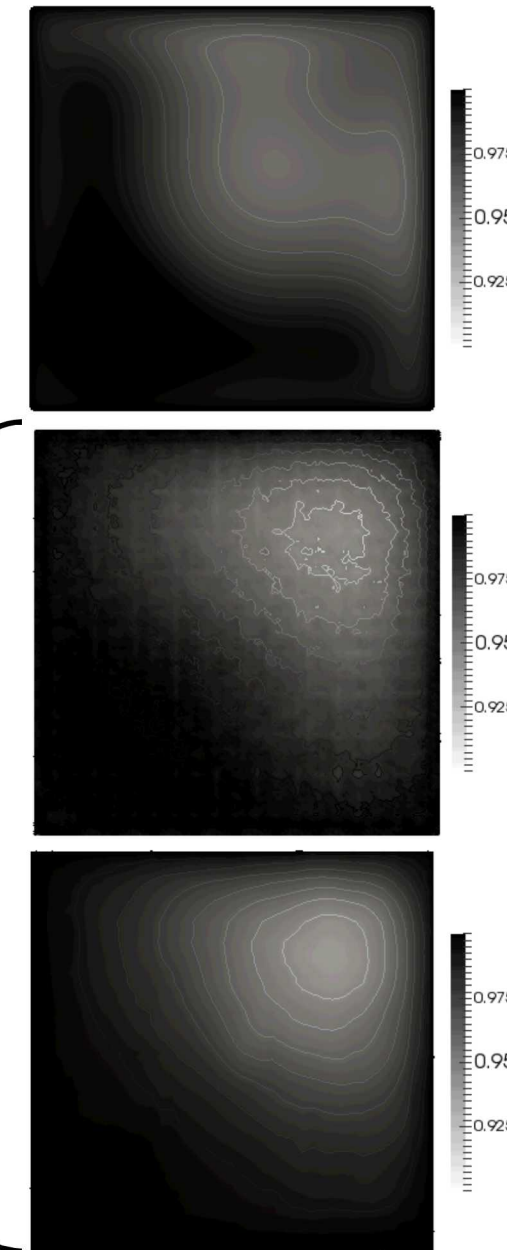
# Results (Transient Advection-Diffusion)

$$\frac{\partial \alpha}{\partial t} = \nabla \cdot (D \nabla \alpha) - \vec{u} \cdot \nabla \alpha$$

$$\alpha(\vec{r}, 0) = 0$$
$$\alpha(\vec{r}, t) = 1 \text{ for } \vec{r} \in \partial\Omega$$



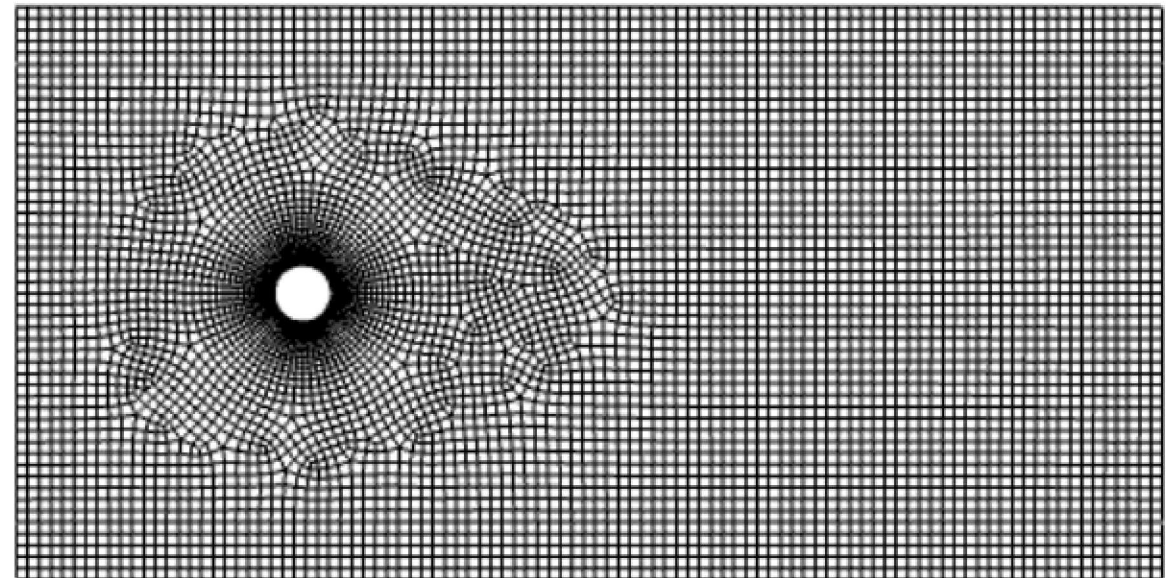
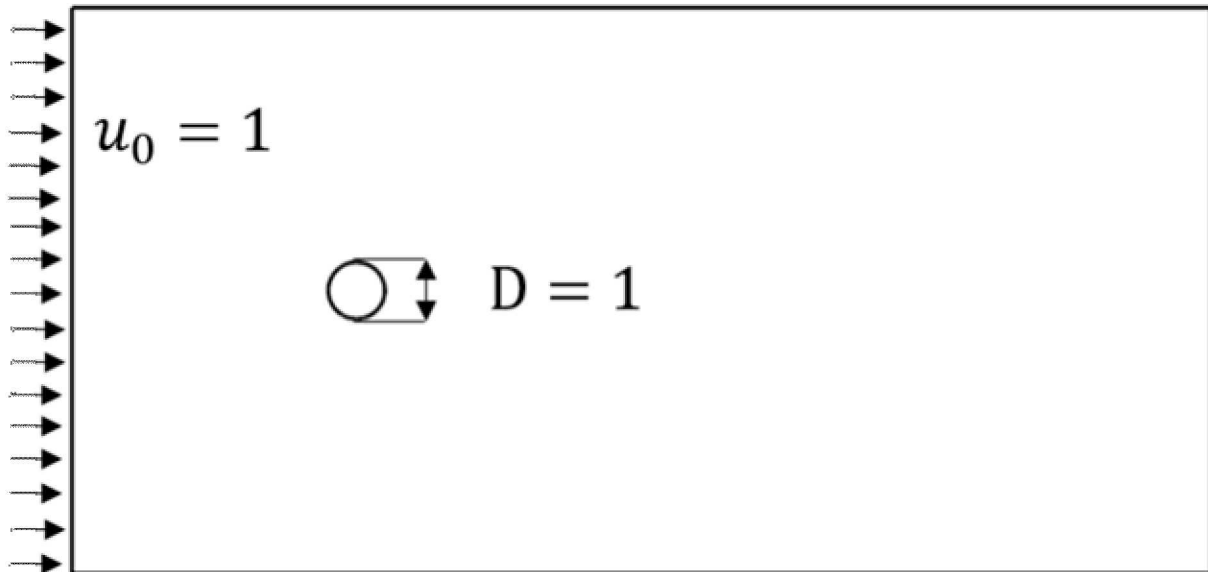
Nonlinear subspace



Traditional CNN

This work

# Results (Incompressible Navier-Stokes)

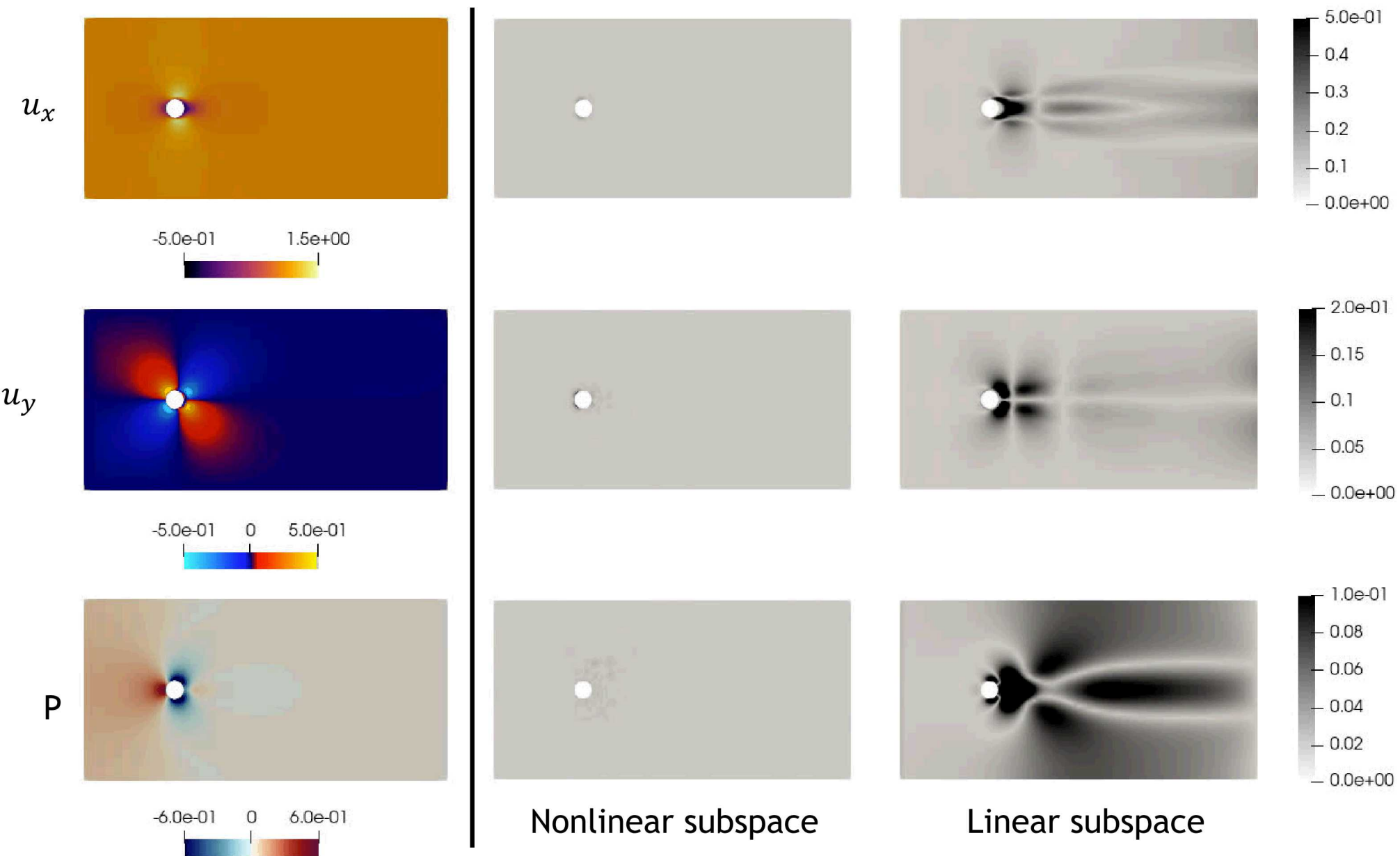


$$\frac{\partial \vec{u}}{\partial t} + (\vec{u} \cdot \nabla) \vec{u} - \nu \nabla^2 \vec{u} = 0$$
$$\nabla \cdot \vec{u} = 0$$

## Results (Navier-Stokes cont'd)

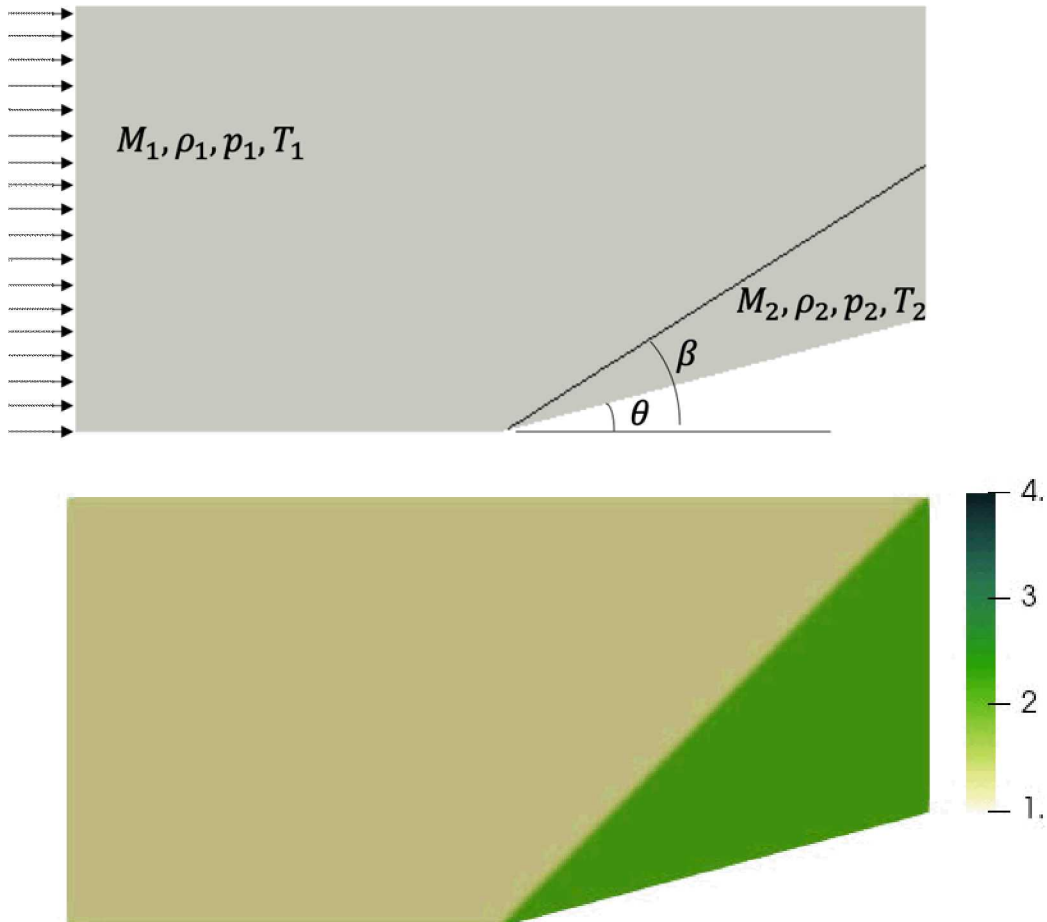


Absolute Reconstruction Error



# Results (Inviscid Euler)

$M_1 = 2.25$



$M_1 \in \{2, 2.1, \dots, 5.9, 6.0\}$

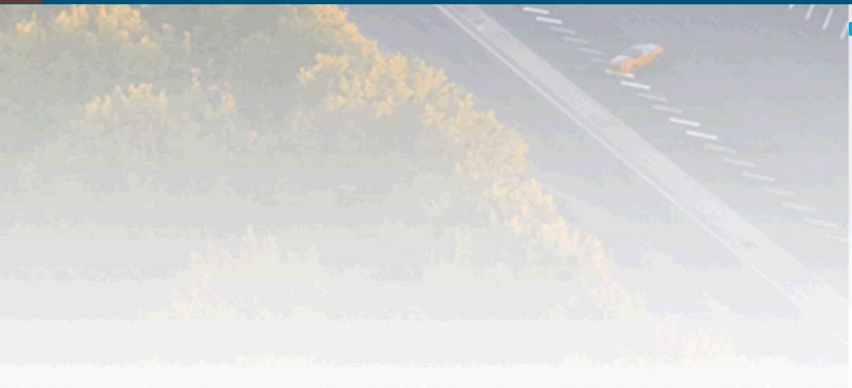


0 0.6

Error in density reconstruction



# Questions?



Supported by the Laboratory Directed Research and Development program at Sandia National Laboratories, a multimission laboratory managed and operated by National Technology and Engineering Solutions of Sandia LLC, a wholly owned subsidiary of Honeywell International Inc. for the U.S. Department of Energy's National Nuclear Security Administration under contract DE-NA0003525.

# Pressio Integration Status



Pressio integration is functional provided:

1. The model is generated/trained using PyTorch exported through TorchVision
2. A finite difference decoder Jacobian is sufficient

I've encountered some difficulties exporting the more complex decoders with TorchVision, so 1 is not a given.

